ACS NANO

www.acsnano.org

ARTICLE

Dissolvable and Recyclable Random Lasers

Xiaoyu Shi,[†] Yu-Ming Liao, Hsia-Yu Lin, Po-Wei Tsao,[‡] Meng-Jer Wu, Shih-Yao Lin, Hsiu-Hao Hu, Zhaona Wang,[†] Tai-Yuan Lin,[‡] Ying-Chih Lai,[§] and Yang-Fang Chen*

Department of Physics, National Taiwan University, Taipei 10617, Taiwan

Supporting Information

ABSTRACT: **An integrated random laser based on green materials with dissolubility and recyclability is created and demonstrated. The dissolvable and recyclable random laser (DRRL) can be dissolved in water, accompanying the decay of emission intensity and the increment in lasing threshold. Furthermore, the DRRL can be reused after the process of deionized treatment, exhibiting excellent reproducibility with several recycling processes.**

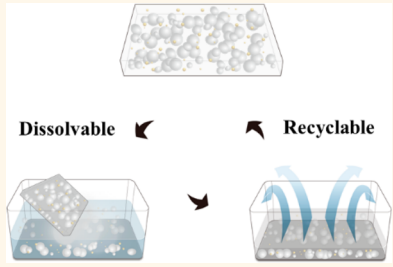

KEYWORDS: *random lasers, dissolvable, recyclable, biocompatible, environmentally sustainable*

The growing requirements of healthcare quality and the rising awareness of environmental protection have sparked a remarkable trend of modern technology modules, which is expected to possess characteristics with biodegradability, biocompatibility, and biometabolizability.[1−4] In the biomedical field, *in vivo* devices are utilized for temporary medical tasks, including localized drug delivery, biointerfaced systems, and point-of-care diagnostics.[5−7] These devices are perceived to cease to function and disappear completely by being metabolized harmlessly in the body at prescribed times and with controlled rates, which could avoid reiterative surgeries for therapeutic device replacement. Furthermore, a tendency nowadays shows that the lifetime of consumer products is becoming shorter and shorter, approaching merely several months. Therefore, it is extremely desirable to design electronic and optical devices that are dissolvable naturally with low impact on the environment, which can help to solve the ecological problem of huge excess waste.

Recently, green inorganic/organic materials such as magnesium, iron, zinc oxide, silicon dioxide, poly(L-lactide-*co*-glycolide) (PLGA), poly(vinyl alcohol) (PVA), silk fibroin, protein, DNA, and gelatin have received adequate attention.[8−14] Toward a sustainable society, optoelectronic devices with transient behavior based on green inorganic/organic materials have created the domain of functionalities and opportunities, which would be inaccessible for the traditional time-invariant design.[8,15,16] Subsequently, great efforts have been made to develop nontoxic, dissolvable, or even recyclable and renewable devices, such as inductors, capacitors, resistors, memristor, transistors, memory, generators, wireless control systems, LEDs, waveguides, *etc.*[16−21] As is well-known, lasers play a very important role in human society, from light sources for communication, images, and sensors to medical treatments,[22−27] including ophthalmology, dermatology, and oncology.[22,23,28] It is believed that lasers incorporated with transient modules can create more applications. However, achieving transient characteristics by traditional lasers can be very challenging, due to the precise optical resonator cavities with meticulous fabrications and special components, for which it may be difficult to find suitable materials to meet the requirements.

Random lasers are good candidates for transient and even recyclable devices. The main reason is that random laser action only needs a disorder system rather than rigid optical cavites to provide feedback loops for the multiple scattering to occur. These features are beneficial for the fabrication of transient random lasers. In addition, such lasing systems have been proven in various materials and applied in diverse fields,[29−36] such as optomicrofluidics,[37] cancer diagnostics,[38] speckle-free imaging,[39] biosensing,[40,41] *etc.* In view of their potential functions especially for biology, development of transient random lasers is greatly needed to promote and broaden *in vivo* or even implantable applications. Furthermore, the random laser device can be easily reproduced and recycled because of the simple design of random lasing systems. In this regard, a device with recyclable functionality and materials can not only reduce the product waste but also save resources of expensive components or substrates, which is a crucial goal in reaching environmental protection and sustainability. Therefore, a concept of transient and recyclable random lasers is proposed here.

The dissolvable and recyclable random laser (DRRL) based on the mixture of semiconductor nanoparticles with water-soluble polymer was designed, fabricated, and demonstrated in this work. Zinc oxide (ZnO) nanoparticles (NPs) as mainly

Received: January 10, 2017
Accepted: June 26, 2017
Published: June 26, 2017

DOI: 10.1021/acsnano.7b00201
ACS Nano 2017, 11, 7600−7607

gain media and titanium dioxide (TiO_2) NPs as the scattering media are embedded into PVA. The DRRL shows very pronounced characteristics of random lasing action operating with a low threshold of 31.3 mJ cm^{-2}. The dissolvable behavior has been studied systematically, revealing the important feature that the DRRL disappears completely in water within 40 min, accompanying the reduction of emission intensity and the increase of laser action threshold. The recycling capability of the DRRL has also been demonstrated by the fact that the active materials of the device are reusable for several times with excellent and reproducible performance. In addition, the DRRL integrated with paper and syringe has also been demonstrated with high performance, showing perfect compatibility to arbitrary substrates.

RESULTS AND DISCUSSION

In our experiment, the DRRL is composed of PVA, TiO_2 NPs, and ZnO NPs, as shown in Figure 1 and Figure S1. PVA, which

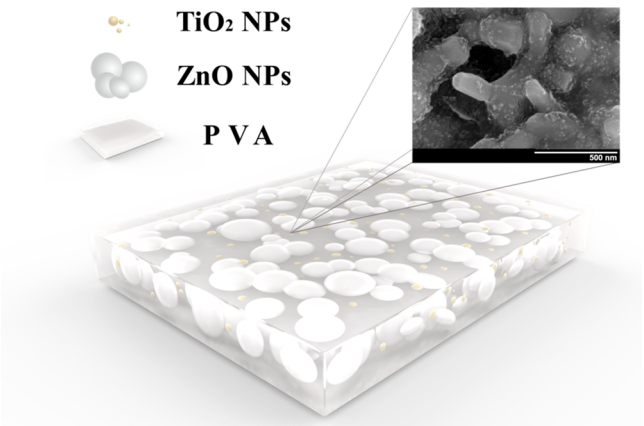

Figure 1. Design of the dissolvable and recyclable random laser (DRRL). Schematic illustration and the scanning electron microscope (SEM) image of the DRRL.

is one of the water-soluble polymers,[42,43] has been used for a variety of biomedical and environmental applications.[9,44−46] It is introduced as the matrix with the scatterers and gain materials packed in it, which is the key to achieving dissolvable devices based on its excellent water-soluble characteristics. ZnO with a wide band gap (3.37 eV) and a high exciton binding energy (60 meV), which is one of the most promising materials for ultraviolet light-emitting sources, serves as the gain material for the random laser device.[31,32] It is worth noting that the refractive index of PVA (n = 1.5) is too close to that of ZnO NPs (n = 1.9); therefore, ZnO NPs cannot act as effective scattering centers. Thus, TiO_2 NPs are chosen as the scatterers to provide a strong confinement and feedback for the random system because their refractive index (n = 2.6) is much larger than that of PVA. Additionally, the ZnO NPs and TiO_2 NPs can help improve the eco-friendly performance because of their high biological compatibility to the environment.[15] The scanning electron microscopy (SEM) image shown in Figure 1 and Figure S1a reveals a highly random structure of the random laser film consisting of ZnO NPs and TiO_2 NPs. The ZnO NPs appear spherical and uniform in the SEM, with diameters of 200−400 nm. The TiO_2 NPs (Figure S1b) reveal an average diameter of 7 nm.

The fundamental working mechanism for random lasing is schematically illustrated in the inset of Figure 2a. When the device is pumped by an external light source, ZnO NPs are excited and emit photons. Because of the refractive index contrast between TiO_2 NPs and PVA/ZnO NPs, the photons undergo multiple scatterings between different scatters, and closed-loop paths can be formed. The behavior of multiple scatterings increases the optical paths in the gain media to obtain enough gain and achieve light amplification. The closed-loop paths increase with the pumping energy density, which serve as cavities for the laser action to occur.[31,32] The lasing threshold and frequencies of different modes are determined by the cavity resonances, resulting in discrete narrow peaks in the emission spectrum.

The emission characteristic of the dissolvable random laser (C_{ZnO} = 750 mg mL^{-1}, C_{TiO_2} = 100 mg mL^{-1}) is systematically demonstrated in Figure 2a by varying the pump energy density. When the pump energy density is at 30.3 mJ cm^{-2}, there is only a broad spontaneous emission band (the black curve in Figure 2a). By increasing the pump energy density above the threshold to 33.7 mJ cm^{-2}, the emission spectrum appears as a narrow emission band centered at 387 nm with several sharp spikes (the red curve in Figure 2a). The line width of the emission band decreases sharply to sub-nanometer. The appearance of the sharp spikes indicates the coherent feedback in a random system,[31] which results from the strong feedback of TiO_2 NPs and large gain provided by ZnO NPs. Figure 2b demonstrates

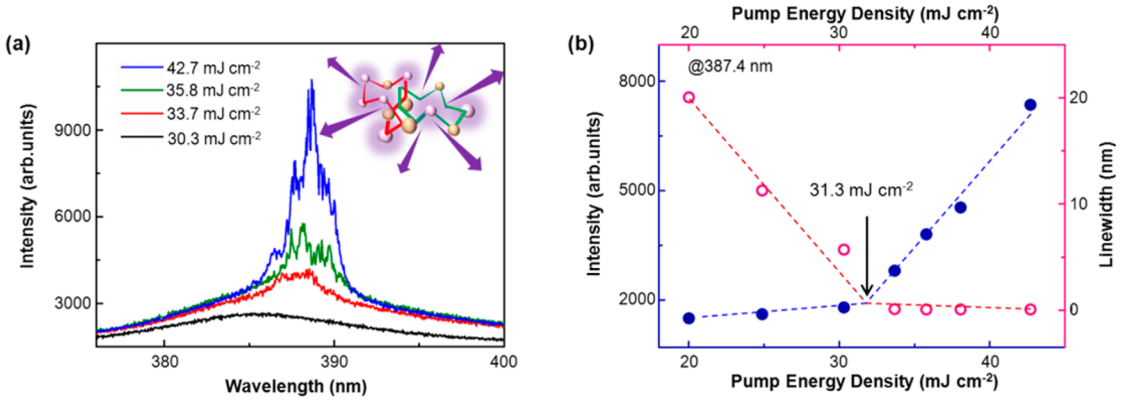

Figure 2. Performance of the dissolvable and recyclable random laser (DRRL). (a) Emission spectra pumped by a 266 nm pulse laser under different pumping energy densities. Inset: Schematic illustration of the working mechanisms responsible for the random laser action in DRRL. (b) Threshold behavior of random lasing with respect to the line width and output intensity from DRRL.

DOI: 10.1021/acsnano.7b00201
ACS Nano 2017, 11, 7600−7607

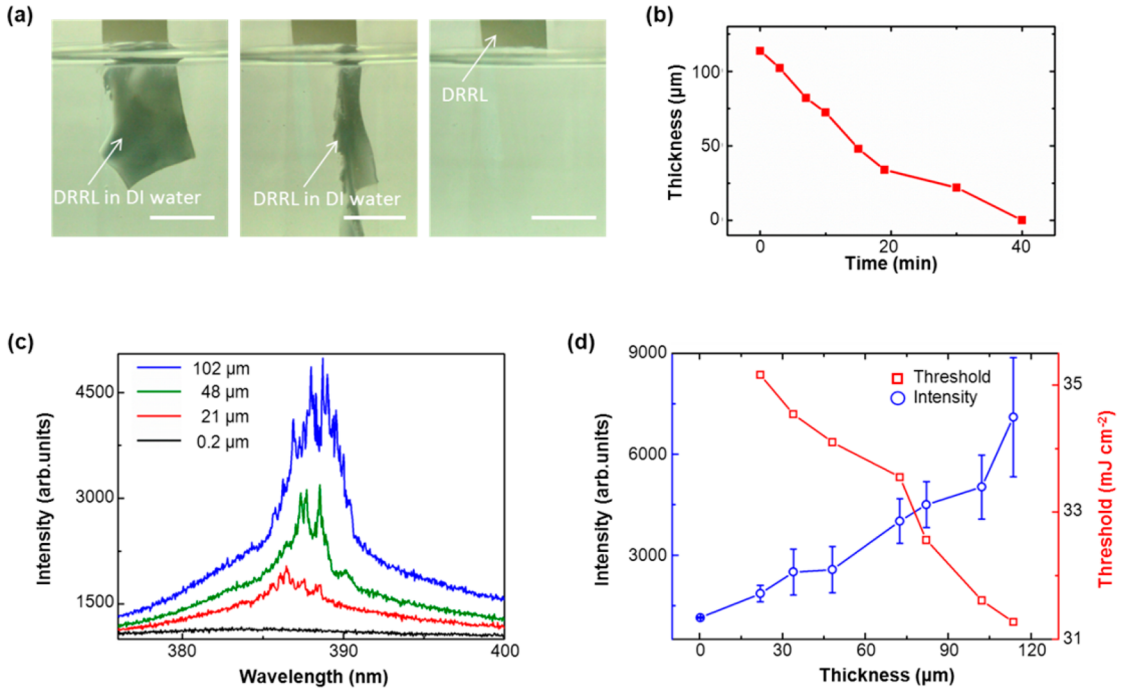

Figure 3. Dissolving performance of the dissolvable and recyclable random laser (DRRL). (a) Photographs at various stages for the DRRL immersed in DI water; the scale bar in the photograph represents 1 cm. (b) Variation of the thickness of the DRRL at various stages of dissolution. (c) Spectra for the DRRL during immersion in DI water at the times of 3, 15, 30, and 40 min. (d) Corresponding evolution of the emission peak intensity and threshold as a function of thickness.

that the line width of the random lasing mode at 387.4 nm (in the red circle of Figure 2b) has a full width at half-maximum (fwhm, $\Delta\lambda$) of 0.08 nm. The corresponding quality factor (defined as $\lambda_{peak}/\Delta\lambda$) is 4843, which is comparable to that of other lasing systems.[35,47] There are more and stronger sharp peaks emerging in the spectrum while further increasing the pump energy density to 35.8 and 42.7 mJ cm^{-2}, as shown by the olive and blue curves shown in Figure 2a. The corresponding maximum emission intensity under each pump energy density and line width of random lasing modes derived from the emission band at 387.4 nm are analyzed in Figure 2b. The threshold of the coherent random lasing is determined to have a value of 31.3 mJ cm^{-2}. Note that according to previous reports,[31,36] the threshold can be determined by the absolute intensity as well as the relative intensity (*i.e.*, the intensity of the spike with deducing the fluorescence background). We have performed both calculations and obtained the same result as shown in Figure S2. When the pump energy densities surpass the threshold, the peak intensities increase rapidly and the line width of the peak decreases sharply with increasing pump energy density. It should be noticed that the spectra transition tends to show a red shift, which can be attributed to the balance between optical gain and self-absorption near the tail of the absorption edge.[48,49] The effects of temperature and band gap renormalization induced red shift can be excluded because after the occurrence of the laser action, the emission spectra only show a slight shift.[48,50] Furthermore, when the incident angle changes from 10 to 80°, coherent random lasing is observed (shown in Figure S3), which is characteristic of random lasers.

More strictly, we then further confirm the mechanism by calculating the closed-loop path. For laser action, the boundary condition of standing waves should be satisfied by the equation[51,52]

$$2nL = M\lambda \quad (1)$$

where n refers to the refractive index of PVA; L is the resonant cavity length; M is a positive integer mode number; and λ is the wavelength (around 385 nm). From this equation, the mode spacing can be calculated by the equation[51,52]

$$\Delta\lambda = \frac{\lambda^2}{2nL} \quad (2)$$

where $\Delta\lambda$ is the spacing between two modes, which is about 3 nm in our random laser spectrum. By the calculation, we can obtain the cavity length about 17 μm, which is close to that in a previous report.[53]

Figure 3 summarizes representative dissolution behavior as a function of time in terms of the change in emission performance of the DRRL. A set of images of the DRRL immersed in DI water at various dissolving stages is presented in Figure 3a. All the films become soft, amorphous, and invisible gradually after soaking in water. The surface layer of the PVA film dissolves rapidly after being immersed in water for a few seconds, and then ZnO NPs and TiO_2 NPs are thereupon found to disperse in water gradually. The image in the middle of Figure 3a shows the dissolved state of the film after several minutes in water. The device completely disappears after 40 min *via* reactive dissolution (the right side of Figure 3a). The corresponding variation of thickness of the film as a function of time exposed to DI water is shown in Figure 3b. The thickness of the device is linearly diminished in water from 113 μm (0 min) to 102 μm (3 min), 82 μm (7 min), 72 μm (10 min), 48 μm (15 min), 33 μm (19 min), 21 μm (30 min) to 0.2 μm (40 min). The emission behaviors responsible for the dissolution of random laser are investigated in Figure 3c and Figure S4. These emission spectra from the random laser for dissolving 3, 15, and 30 min exhibit several spikes arising from coherent random

DOI: 10.1021/acsnano.7b00201
ACS Nano 2017, 11, 7600−7607

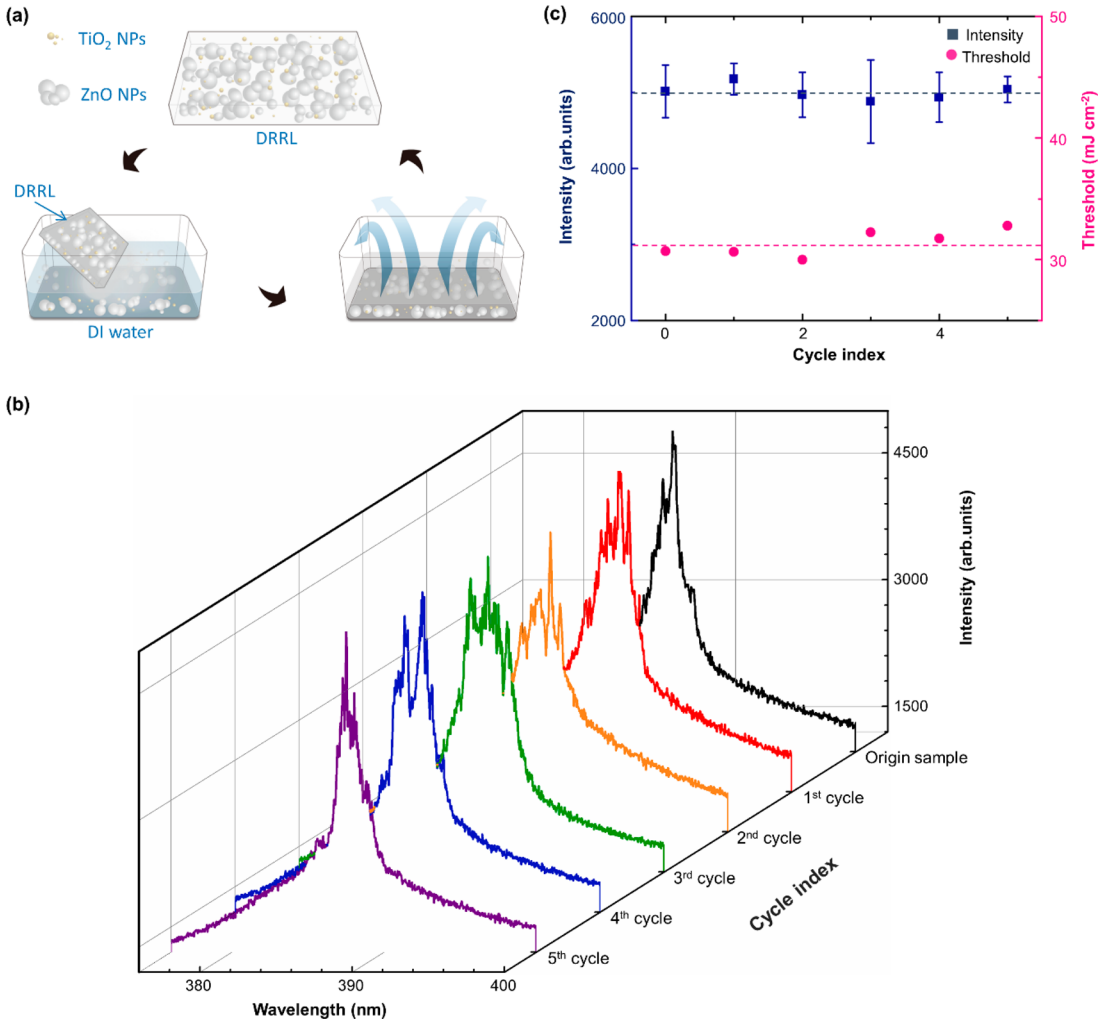

Figure 4. Recycling and reusable performance of the dissolvable and recyclable random laser (DRRL). (a) Schematic illustration of the recycling process. (b) Emission spectra with different cycle index. (c) Corresponding evolution of emission peak intensity and threshold as a function of recycling times.

lasing with a line width of ~0.08 nm around 387 nm. These spikes demonstrate the typical lasing behavior when the pump energy density exceeds 31.2, 34.1, and 35.2 mJ cm^{-2}, respectively (see Figure S5). After being immersed for 40 min, the weak spontaneous emission from the sample centered at 387 nm is observed. Random laser action cannot be observed even when the pump energy density is increased to 85.6 mJ cm^{-2}. Threshold behavior at the dissolving times of 7, 10, and 19 min is described in Figure S5. The decrease of ZnO NPs and TiO_2 NPs in the film during the dissolving process results in the changes of gain and scattering loops. The random laser intensity and threshold are consequently changed. The corresponding evolution of the emission peak intensity and threshold as a function of thickness are shown in Figure 3d. The peak intensities under the pumping energy density of 35.8 mJ cm^{-2} for representative devices are 5025 ± 952, 2569 ± 684, 1902 ± 233, and 1165 ± 18 for dissolving time of 3, 15, 30, and 40 min, respectively. The intensity changes by ~29, 63, 73, and 84% during immersion for 3, 15, 30, and 40 min, respectively. This dissolution behavior is consistent with the variation of the emission property while changing the thickness of the random laser film (Figure S6). Furthermore, the change of the ZnO/TiO_2 nanoparticles accompanies the dissolving time (Figure S7), contributing to the increase of the threshold and the decrease of the emission intensity. The measured peak intensity (red dots) and lasing threshold (blue dots) show stable operation for 10−30 min, followed by rapid degradation over the next 10 min. The threshold increases around 12% during the dissolution process. The dissolvable behavior of the random lasers demonstrates that the PVA-based design can be implanted *in vivo* as a transient light source for clinical treatment. Moreover, the developed environmentally friendly optoelectronic systems are very useful to minimize the dramatic increase of consumer product waste for pursuing environmental sustainability.

Next, the distinct feedback mechanism based on a disorder structure gives the possibility of refabrication of the active materials for recycled lasers. Figure 4a shows the recycle process for the DRRL to test for its recycling potential. Once the DRRL is dissolved in water, isolated intact ZnO NPs and TiO_2 NPs can be seen after being dissolved completely after 40 min, which can be rearranged by evaporating water. Then the refabricated DRRL can be dissolved again after use. The corresponding experimentally characterized photograph of the DRRL devices can be seen in Figure S8. A set of spectra pumped at 35.8 mJ cm^{-2} (seen in Figure 4b) shows the emission properties of random lasers with different cycle index under the same conditions, indicating that no significant

DOI: 10.1021/acsnano.7b00201
ACS Nano 2017, 11, 7600−7607

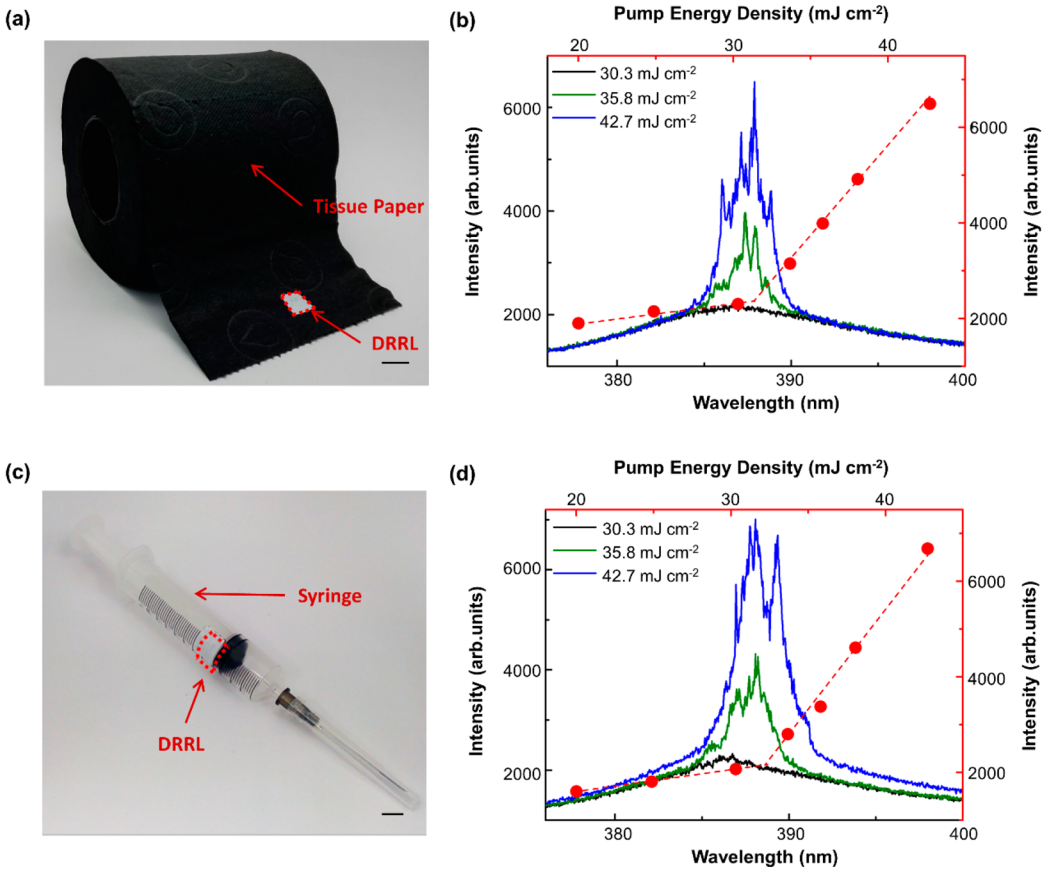

Figure 5. Demonstration of the dissolvable and recyclable random laser (DRRL). (a) Photograph and (b) emission spectra from the DRRL on a piece of tissue paper. (c) Photograph and (d) emission spectra from the DRRL on a syringe. The scale bar in the photograph represents 1 cm.

variation is observed. The corresponding evolution of emission peak intensity and threshold (see details in Figure S9) as a function of cycle index are shown in Figure 4c, indicating a stable output with a slight fluctuation. As these nanoparticles embedded into PVA may induce subsequent change in the structure related to feedback channels for coherent lasing, there are slight fluctuations in spectral intensity and threshold for the recycled samples. Herein, from the results for recycling of the active materials of the random laser, we find that the random laser can be easily re-formed because of its special structure and feedback mechanism. After five cycles of recycling, the DRRL still shows constant emission intensity, thereby demonstrating the possibility of recycling random lasers. The time durations for stable operation reported here establish avenues for random systems that have the capability to be cyclically utilized and to save precious resources. Moreover, the results also indicate that the substrate can be reused after the whole device package is dissolved by water. Furthermore, the stability of new device and recycled device has been investigated, as shown in Figure S10, which demonstrates excellent stability of our device. Hence the scatterers, gain materials, and substrates of random lasers can be reused. These characteristics are particularly important in applications that involve integration with transient devices. These advantages are exactly up to the standards of a recycling-based society, advocating action plans for reducing the generation of waste, reuse of materials, recycling, and appropriate disposal of waste.[2,3,54] The methodology used here, to establish that the random lasers could be dissolved and recycled, can be extended to many other optoelectronic devices.

To put our concept into practice, we integrated the DRRLs with daily one-off items such as tissue paper and medical supplies. First, we transferred the DRRL onto a piece of tissue paper. Figure 5a presents a schematic illustration of the DRRL on the tissue paper. The results in Figure 5b represent the emission spectra of the random laser with sharp peaks around 387 nm, which indicate the building of coherent feedback. The threshold behavior of this system is shown by the red dots in Figure 5b, revealing that its threshold is about 31.2 mJ cm^{-2}. Hence, we can conclude that the DRRL can also be transferred to other environmentally friendly substrates, such as silk and biological tissues. Lasing signal can be easily obtained on these rigid, flexible, nonplanar, and rough substrates to avoid unsuitable fabricating processes. The report provides a framework for further research on eco-friendly random lasers, which can be used as short period source units implanted in military equipment or used in transient environmental sensors. Biomedicine applications like medical apparatus and instruments are another key demand for such transient and recyclable random laser devices for waste reduction. We have transferred the DRRL onto a syringe, as shown in Figure 5c. The spectra in Figure 5d show several spikes centered around 387 nm with a threshold of about 32.5 mJ cm^{-2} at 388.4 nm (see the red dots in Figure 5d). It shows that the DRRL functioned well, which offers a great opportunity for developing the identification labels in a low-cost and easy method. Moreover, transient random lasers not only reduce the waste but also help sterilize the waste for the bactericidal effect of ZnO NPs and TiO_2 NPs. From the above demonstrations, potential applications of the

DOI: 10.1021/acsnano.7b00201
ACS Nano 2017, 11, 7600−7607

degradable optoelectronic devices range from biodegradable substrates to one-off medical devices.

CONCLUSION

A transient and recyclable random laser is proposed and fabricated based on ZnO NPs and TiO_2 NPs mixed into PVA as an environmentally friendly coherent lasing source. The distinct behavior of random laser action operating with a low threshold of 31.3 mJ cm^{-2} is obtained. The dissolution process has been described in detail with the corresponding characteristics of laser spectra under different immersion times in DI water. It is found that the DRRL can be dissolved completely in DI water within 40 min owing to the dissolvable property of PVA, accompanying the reduction of emission intensity and the increase of laser action threshold. The recycled experiments illustrate that excellent reproducibility can be achieved by the DRRL. Tissue paper and syringe-based transient random lasers provide two application examples of the eco-friendly behaviors of the DRRL.

METHODS

Preparation of the DRRL. In our experiment, high-purity ZnO powders (n = 1.9), PVA (n = 1.52), and TiO_2 (n = 2.6) powders were used directly without further purification. First, PVA was dissolved into deionized (DI) water with a mass fraction of 5 wt % and stirred for 30 min at room temperature. A total of 150 mg of high-purity ZnO NPs (99.99%) and 1 mL of TiO_2 aqueous solution (with a concentration of 20 mg mL^{-1}) were added into a 4 mL PVA colloidal solution and sonicated for 30 min to obtain a homogeneous solution mixture. The silicon substrates (1.5 cm × 1.5 cm) were ultrasonically cleaned for 10 min in DI water, acetone, and isopropyl alcohol to remove any absorbed contaminant. After the treatment, the poly(methyl methacrylate) (PMMA) solution was first spin-coated on the silicon substrates at a rate of 800 rpm for 60 s and dried at 85 °C. The mixture solution was dropped stepwise on the silicon substrates. It was then heated at 80 °C for 20 min to evaporate unnecessary DI water. Finally, to separate the PVA based film from the silicon substrates, we soaked the device in acetone to dissolve the PMMA layer. Thus, the PVA layer was floating on the surface of water (seen in Figure S11). After being separated from the silicon wafer, the DRRL was then transferred onto more flexible and curving substrates, such as paper and the syringe. First, we dipped some PVA solution on one side of the film and then transferred the film onto the surface of the paper or the syringe. The film can stick to paper and the syringe very well.

Material Characterization. The microscopic structures of the random laser film were characterized by SEM (Hitachi S4800 microscope).

Optical Measurement. The DRRLs were optically excited by a Q-switched fourth harmonic Nd:YAG laser (266 nm, 3−5 ns pulse, 10 Hz) and measured with a Jobin Yvon iHR550 imaging spectrometer system. The laser beam was focused on the DRRLs with a diameter of about 200 μm. All the experiments were conducted at room temperature.

Dissolving Experiment of Environmentally Friendly Random Lasing Systems. In this experiment, the thickness measurement was conducted on the dried samples. We prepared eight pieces of samples with the same conditions. To test the dissolvability and environmental protection property, we immersed seven pieces of samples in DI water at room temperature. The samples were dissolved with different times of 3, 7, 10, 15, 19, 30, and 40 min. After being taken out from the water at various stages of the dissolution, the samples were dried at 80 °C for 20 min to remove the residual water.

Recycle Experiment of the DRRL. To test the recycling capability, the prepared DRRL was immersed ultrasonically in 1 mL of DI water until the film was totally dissolved at room temperature. Next, all the solutions were dropped on the silicon substrates and dried at 80 °C to remove the residual water. After the emission property was recorded, the DRRL was dissolved again and the steps as described above were repeated.

ASSOCIATED CONTENT

Supporting Information

The Supporting Information is available free of charge on the ACS Publications website at DOI: 10.1021/acsnano.7b00201.

Characterization of ZnO nanoparticles and TiO_2 nanoparticles; comparison of threshold for the DRRL by absolute intensity and relative intensity; emission spectra of the DRRL taken from different incident angles; spectra and threshold characteristics of the DRRL under different dissolving time; characterization for the DRRL with different thicknesses; surface topography of the DRRL device during the dissolve process; characterization photograph of the DRRL in the recycle process; threshold behavior of the DRRL with different repeating cycles; stability of the DRRL; and photograph of the DRRL in the recycle process (PDF)

AUTHOR INFORMATION

Corresponding Author

*E-mail: yfchen@phys.ntu.edu.tw.

ORCID

Yu-Ming Liao: 0000-0002-8696-7313

Present Addresses

[†]Applied Optics Beijing Area Major Laboratory, Department of Physics, Beijing Normal University, Beijing 100875, China.
[‡]Institute of Optoelectronic Sciences, National Taiwan Ocean University, Keelung 202, Taiwan.
[§]Department of Materials Science and Engineering, National Chung Hsing University, Taichung 40227, Taiwan.

Author Contributions

X.S. and Y.-M.L. contributed equally to this work. X.S. and Y.-M.L. designed the experiments and performed the experiments. H.-Y.L, T.-Y.L., M.-J.W., S.-Y.L., H.-H.H., and P.-W.T. helped to solve technical problem. Y.-C.L. provided the idea. X.S., Y.-M.L., Z.W., and Y.-F.C. wrote the paper. Y.-F.C. supervised the project and conceived the study.

Notes

The authors declare no competing financial interest.

ACKNOWLEDGMENTS

This work was supported by the Ministry of Science and Technology and Ministry of Education of the Republic of China.

REFERENCES

(1) Irimia-Vladu, M.; Głowacki, E. D.; Voss, G.; Bauer, S.; Sariciftci, N. S. Green and Biodegradable Electronics. *Mater. Today* **2012**, *15*, 340−346.

(2) Larcher, D.; Tarascon, J. M. Towards Greener and More Sustainable Batteries for Electrical Energy Storage. *Nat. Chem.* **2014**, *7*, 19−29.

(3) Kim, B. J.; Kim, D. H.; Kwon, S. L.; Park, S. Y.; Li, Z.; Zhu, K.; Jung, H. S. Selective Dissolution of Galide Perovskites As A Step towards Recycling Solar Cells. *Nat. Commun.* **2016**, *7*, 11735.

(4) Irimia-Vladu, M.; Troshin, P. A.; Reisinger, M.; Schwabegger, G.; Ullah, M.; Schwoediauer, R.; Mumyatov, A.; Bodea, M.; Fergus, J. W.; Razumov, V. F. Environmentally Sustainable Organic Field Effect Transistors. *Org. Electron.* **2010**, *11*, 1974−1990.

DOI: 10.1021/acsnano.7b00201
ACS Nano 2017, 11, 7600−7607

(5) Irimia-Vladu, M.; Troshin, P. A.; Reisinger, M.; Shmygleva, L.; Kanbur, Y.; Schwabegger, G.; Bodea, M.; Schwödiauer, R.; Mumyatov, A.; Fergus, J. W.; Razumov, V. F.; Sitter, H.; Sariciftci, N. S.; Bauer, S. Biocompatible and Biodegradable Materials for Organic Field-Effect Transistors. *Adv. Funct. Mater.* **2010**, *20*, 4069−4076.
(6) Kim, D.-H.; Viventi, J.; Amsden, J. J.; Xiao, J.; Vigeland, L.; Kim, Y.-S.; Blanco, J. A.; Panilaitis, B.; Frechette, E. S.; Contreras, D.; Kaplan, D. L.; Omenetto, F. G.; Huang, Y.; Hwang, K.-C.; Zakin, M. R.; Litt, B.; Rogers, J. A. Dissolvable Films of Silk Fibroin for Ultrathin Conformal Bio-integrated Electronics. *Nat. Mater.* **2010**, *9*, 511−517.
(7) Boutry, C. M.; Nguyen, A.; Lawal, Q. O.; Chortos, A.; Rondeau-Gagné, S.; Bao, Z. A Sensitive and Biodegradable Pressure Sensor Array for Cardiovascular Monitoring. *Adv. Mater.* **2015**, *27*, 6954−6961.
(8) Yin, L.; Cheng, H.; Mao, S.; Haasch, R.; Liu, Y.; Xie, X.; Hwang, S.-W.; Jain, H.; Kang, S.-K.; Su, Y.; Li, R.; Huang, Y.; Rogers, J. A. Dissolvable Metals for Transient Electronics. *Adv. Funct. Mater.* **2014**, *24*, 645−658.
(9) Bettinger, C. J.; Bao, Z. Organic Thin-film Transistors Fabricated on Resorbable Biomaterial Substrates. *Adv. Mater.* **2010**, *22*, 651−655.
(10) Hota, M. K.; Bera, M. K.; Kundu, B.; Kundu, S. C.; Maiti, C. K. A Natural Silk Fibroin Protein-based Transparent Bio-Memristor. *Adv. Funct. Mater.* **2012**, *22*, 4493−4499.
(11) Wang, H.; Meng, F.; Cai, Y.; Zheng, L.; Li, Y.; Liu, Y.; Jiang, Y.; Wang, X.; Chen, X. Sericin for Resistance Switching Device with Multilevel Nonvolatile Memory. *Adv. Mater.* **2013**, *25*, 5498−5503.
(12) Chen, Y.-S.; Hong, M.-Y.; Huang, G. S. A Protein Transistor Made of An Antibody Molecule and Two Gold Nanoparticles. *Nat. Nanotechnol.* **2012**, *7*, 197−203.
(13) Hung, Y.-C.; Hsu, W.-T.; Lin, T.-Y.; Fruk, L. Photoinduced Write-once Read-many-times Memory Device Based on DNA Biopolymer Nanocomposite. *Appl. Phys. Lett.* **2011**, *99*, 253301.
(14) Chang, Y. C.; Wang, Y. H. Resistive Switching Behavior in Gelatin Thin Films for Nonvolatile Memory Application. *ACS Appl. Mater. Interfaces* **2014**, *6*, 5413−5421.
(15) Dagdeviren, C.; Hwang, S. W.; Su, Y.; Kim, S.; Cheng, H.; Gur, O.; Haney, R.; Omenetto, F. G.; Huang, Y.; Rogers, J. A. Transient, Biocompatible Electronics and Energy Harvesters Based on ZnO. *Small* **2013**, *9*, 3398−3404.
(16) Hwang, S.-W.; Kim, D.-H.; Tao, H.; Kim, T.-i.; Kim, S.; Yu, K. J.; Panilaitis, B.; Jeong, J.-W.; Song, J.-K.; Omenetto, F. G.; Rogers, J. A. Materials and Fabrication Processes for Transient and Bioresorbable High-Performance Electronics. *Adv. Funct. Mater.* **2013**, *23*, 4087−4093.
(17) Hosseini, N. R.; Lee, J.-S. Biocompatible and Flexible Chitosan-based Resistive Switching Memory with Magnesium Electrodes. *Adv. Funct. Mater.* **2015**, *25*, 5586−5592.
(18) Zheng, Q.; Zou, Y.; Zhang, Y.; Liu, Z.; Shi, B.; Wang, X.; Jin, Y.; Ouyang, H.; Li, Z.; Wang, Z. L. Biodegradable Triboelectric Nanogenerator As A Life-time Designed Implantable Power Source. *Sci. Adv.* **2016**, *2*, e1501478.
(19) Boutry, C. M.; Chandrahalim, H.; Streit, P.; Schinhammer, M.; Hanzi, A. C.; Hierold, C. Towards Biodegradable Wireless Implants. *Philos. Trans. R. Soc., A* **2012**, *370*, 2418−2432.
(20) Zhu, H.; Xiao, Z.; Liu, D.; Li, Y.; Weadock, N. J.; Fang, Z.; Huang, J.; Hu, L. Biodegradable Transparent Substrates for Flexible Organic-light-emitting Diodes. *Energy Environ. Sci.* **2013**, *6*, 2105.
(21) Kim, D. H.; Viventi, J.; Amsden, J. J.; Xiao, J.; Vigeland, L.; Kim, Y. S.; Blanco, J. A.; Panilaitis, B.; Frechette, E. S.; Contreras, D.; Kaplan, D. L.; Omenetto, F. G.; Huang, Y.; Hwang, K. C.; Zakin, M. R.; Litt, B.; Rogers, J. A. Dissolvable Films of Silk Fibroin for Ultrathin Conformal Bio-integrated Electronics. *Nat. Mater.* **2010**, *9*, 511−517.
(22) Fan, X.; Yun, S.-H. The Potential of Optofluidic Biolasers. *Nat. Methods* **2014**, *11*, 141−147.
(23) Khan, I.; Tang, E.; Arany, P. Molecular Pathway of Near-infrared Laser Phototoxicity Involves ATF-4 Orchestrated ER Stress. *Sci. Rep.* **2015**, *5*, 10581.
(24) Liu, T.-M.; Conde, J.; Lipiński, T.; Bednarkiewicz, A.; Huang, C.-C. Revisiting the Classification of NIR-absorbing/emitting Nanomaterials for *in vivo* Bioapplications. *NPG Asia Mater.* **2016**, *8*, e295.
(25) Chen, Q.; Xu, L.; Liang, C.; Wang, C.; Peng, R.; Liu, Z. Photothermal Therapy with Immune-adjuvant Nanoparticles Together with Checkpoint Blockade for Effective Cancer Immunotherapy. *Nat. Commun.* **2016**, *7*, 13193.
(26) Wu, E. C.; Wong, B. F. Lasers and Optical Technologies in Facial Plastic Surgery. *JAMA Facial Plast. Surg.* **2008**, *10*, 381−390.
(27) Zemelman, B. V.; Lee, G. A.; Ng, M.; Miesenböck, G. Selective Photostimulation of Genetically ChARGed Neurons. *Neuron* **2002**, *33*, 15−22.
(28) Marago, O. M.; Jones, P. H.; Gucciardi, P. G.; Volpe, G.; Ferrari, A. C. Optical Trapping and Manipulation of Nanostructures. *Nat. Nanotechnol.* **2013**, *8*, 807−819.
(29) Lawandy, N. M.; Balachandran, R. M.; Gomes, A. S. L.; Sauvain, E. Laser Action in Strongly Scattering Media. *Nature* **1994**, *368*, 436−438.
(30) Frolov, S. V.; Gellermann, W.; Ozaki, M.; Yoshino, K.; Vardeny, Z. V. Cooperative Emission in π-conjugated Polymer Thin Films. *Phys. Rev. Lett.* **1997**, *78*, 729−732.
(31) Cao, H.; Zhao, Y. G.; Ho, S. T.; Seelig, E. W.; Wang, Q. H.; Chang, R. P. H. Random Laser Action in Semiconductor Powder. *Phys. Rev. Lett.* **1999**, *82*, 2278−2281.
(32) Cao, H. Review on Latest Developments in Random Lasers with Coherent Feedback. *J. Phys. A: Math. Gen.* **2005**, *38*, 10497−10535.
(33) Gottardo, S.; Sapienza, R.; García, P. D.; Blanco, A.; Wiersma, D. S.; López, C. Resonance-driven Random Lasing. *Nat. Photonics* **2008**, *2*, 429−432.
(34) Cao, H.; Xu, J. Y.; Zhang, D. Z.; Chang, S. H.; Ho, S. T.; Seelig, E. W.; Liu, X.; Chang, R. P. H. Spatial Confinement of Laser Light in Active Random Media. *Phys. Rev. Lett.* **2000**, *84*, 5584−5587.
(35) Shi, X.; Wang, Y.; Wang, Z.; Wei, S.; Sun, Y.; Liu, D.; Zhou, J.; Zhang, Y.; Shi, J. Random Lasing with A High Quality Factor over The Whole Visible Range Based on Cascade Energy Transfer. *Adv. Opt. Mater.* **2014**, *2*, 88−93.
(36) Zhai, T.; Zhang, X.; Pang, Z.; Su, X.; Liu, H.; Feng, S.; Wang, L. Random Laser Based on Waveguided Plasmonic Gain Channels. *Nano Lett.* **2011**, *11*, 4295−8.
(37) Viola, I.; Ghofraniha, N.; Zacheo, A.; Arima, V.; Conti, C.; Gigli, G. Random Laser Emission from A Paper-based Device. *J. Mater. Chem. C* **2013**, *1*, 8128.
(38) Polson, R. C.; Vardeny, Z. V. Random Lasing in Human Tissues. *Appl. Phys. Lett.* **2004**, *85*, 1289−1291.
(39) Redding, B.; Choma, M. A.; Cao, H. Speckle-free Laser Imaging Using Random Laser Illumination. *Nat. Photonics* **2012**, *6*, 355−359.
(40) Song, Q.; Xiao, S.; Xu, Z.; Liu, J.; Sun, X.; Drachev, V.; Shalaev, V. M.; Akkus, O.; Kim, Y. L. Random Lasing in Bone Tissue. *Opt. Lett.* **2010**, *35*, 1425−1427.
(41) Ignesti, E.; Tommasi, F.; Fini, L.; Martelli, F.; Azzali, N.; Cavalieri, S. A New Class of Optical Sensors: A Random Laser Based Device. *Sci. Rep.* **2016**, *6*, 35225.
(42) Zhai, T.; Chen, J.; Chen, L.; Wang, J.; Wang, L.; Liu, D.; Li, S.; Liu, H.; Zhang, X. A Plasmonic Random Laser Tunable Through Stretching Silver Nanowires Embedded in A Flexible Substrate. *Nanoscale* **2015**, *7*, 2235−2240.
(43) Kushto, G. P.; Kim, W.; Kafafi, Z. H. Flexible Organic Photovoltaics Using Conducting Polymer Electrodes. *Appl. Phys. Lett.* **2005**, *86*, 093502.
(44) Ferreira, L. S.; Gerecht, S.; Fuller, J.; Shieh, H. F.; Vunjak-Novakovic, G.; Langer, R. Bioactive Hydrogel Scaffolds for Controllable Vascular Differentiation of Human Embryonic Stem Cells. *Biomaterials* **2007**, *28*, 2706−2717.
(45) Chiellini, E.; Corti, A.; D'Antone, S.; Solaro, R. Biodegradation of Poly (vinyl alcohol) Based Materials. *Prog. Polym. Sci.* **2003**, *28*, 963−1014.
(46) Gaaz, T. S.; Sulong, A. B.; Akhtar, M. N.; Kadhum, A. A.; Mohamad, A. B.; Al-Amiery, A. A. Properties and Applications of

DOI: 10.1021/acsnano.7b00201
ACS Nano 2017, 11, 7600−7607

Polyvinyl Alcohol, Halloysite Nanotubes and Their Nanocomposites. *Molecules* **2015**, *20*, 22833−22847.
(47) Gambetta, J.; Blais, A.; Boissonneault, M.; Houck, A. A.; Schuster, D. I.; Girvin, S. M. Quantum Trajectory Approach to Circuit QED: Quantum Jumps and The Zeno Effect. *Phys. Rev. A: At., Mol., Opt. Phys.* **2008**, *77*, 012112.
(48) Ding, J.; Hagerott, M.; Ishihara, T.; Jeon, H.; Nurmikko, A. V. Zn,Cd)Se/ZnSe Quantum-well Lasers: Excitonic Gain in An Inhomogeneously Broadened Quasi-two-dimensional System. *Phys. Rev. B: Condens. Matter Mater. Phys.* **1993**, *47*, 10528−10542.
(49) Perumal, P.; Wang, C.-S.; Boopathi, K. M.; Haider, G.; Liao, W.-C.; Chen, Y.-F. Whispering Gallery Mode Lasing from Self-assembled Hexagonal Perovskite Single Crystals and Porous Thin Films Decorated by Dielectric Spherical Resonators. *ACS Photonics* **2017**, *4*, 146−155.
(50) Zu, P.; Tang, Z. K.; Wong, G. K. L.; Kawasaki, M.; Ohtomo, A.; Koinuma, H.; Segawa, Y. Ultraviolet Spontaneous and Stimulated Emissions from ZnO Microcrystallite Thin Films at Room Temperature. *Solid State Commun.* **1997**, *103*, 459−463.
(51) Nathan, M. I.; Fowler, A. B.; Burns, G. Oscillations in GaAs Spontaneous Emission in Fabry-Perot Cavities. *Phys. Rev. Lett.* **1963**, *11*, 152−154.
(52) Chen, Y. L.; Chen, C. L.; Lin, H. Y.; Chen, C. W.; Chen, Y. F.; Hung, Y.; Mou, C. Y. Enhancement of Random Lasing Based on The Composite Consisting of Nanospheres Embedded in Nanorods Template. *Opt. Express* **2009**, *17*, 12706−12713.
(53) Wang, C.-S.; Nieh, C.-H.; Lin, T.-Y.; Chen, Y.-F. Electrically Driven Random Laser Memory. *Adv. Funct. Mater.* **2015**, *25*, 4058−4063.
(54) Nishida, H. Development of Materials and Technologies for Control of Polymer Recycling. *Polym. J.* **2011**, *43*, 435−447.

DOI: 10.1021/acsnano.7b00201
ACS Nano 2017, 11, 7600−7607